J Mol Model (2015) 21: 209
DOI 10.1007/s00894-015-2750-x

ORIGINAL PAPER

Superalkali atoms bonding to the phenalenyl radical: structures, intermolecular interaction and nonlinear optical properties

Sa Chen[1] · **Hong-Liang Xu**[1] · **Shi-Ling Sun**[1] · **Liang Zhao**[1] · **Zhong-Min Su**[1]

Received: 5 February 2015 / Accepted: 3 July 2015 / Published online: 28 July 2015

Abstract Due to unpaired electrons, both radicals and superalkali are investigated widely. In this work, two interesting complexes (Li_3O-PLY and Li_3-PLY) were constructed by phenalenyl radical and superalkali atoms. Why are they interesting? Firstly, for Li_3O-PLY and Li_3-PLY, although the charge transfer between superalkali atoms and PLY is similar, the sandwich-like charge distribution for Li_3O-PLY causes a smaller dipole moment than that of Li_3-PLY. Secondly, their UV–vis absorption show that the maximum wavelengths for Li_3O-PLY and Li_3-PLY display a bathochromic shift compared to PLY. Moreover, Li_3-PLY has two new peaks at 482 and 633 nm. Significantly, the β_0 values of Li_3-PLY (4943–5691 a.u.) are much larger than that of Li_3O-PLY (225–347 a.u.). Further, the β_{HRS} values of Li_3O-PLY decrease slightly while β_{HRS} of Li_3-PLY increase dramatically with increasing frequency. It is our expectation that these results might provide beneficial information for theoretical and experimental studies on complexes with superalkali and PLY radicals.

Keywords Superalkali · Radical · Interaction energy · First hyperpolarizability · UV–vis absorption

✉ Hong-Liang Xu
hlxu@nenu.edu.cn

✉ Shi-Ling Sun
sunsl430@nenu.edu.cn

[1] Institute of Functional Materials Chemistry, Faculty of Chemistry, Northeast Normal University, Changchun 130024, Jilin, People's Republic of China

Introduction

Phenalenyl (PLY) radicals, considered as the building blocks for the assembly of novel molecule-based conductors and magnets, have attracted much attention from both theorists [1–5] and experimentalists [6–10]. For example, in 2006, Morita and coworkers [1] investigated the CSI-MS and NMR spectra of tri-tert-butylated biphenalenyl π-dimers for the first time. In 1999, Haddon and coworkers [6] reported the characterization of spiro-biphenalenyl radical—the first phenalenyl-based neutral radical molecular conductor. The phenalenyl radical consists of three adjacent benzene rings that share a central carbon atom with a highly symmetrical structure. (see Scheme 1)

On the other hand, superatom families have generated a great deal of theoretical [11–16] and experimental [17, 18]interest. Particularly, an important class of superatoms are superalkalis, which act as potential building blocks for nanostructural materials [19, 20]. Superalkalis have lower ionization potentials (IPs) than those (5.4–3.9 eV) of alkali atoms, which serve as stronger electron donors. In 1978, Kudo et al. [21] found the first hyperlithiated molecule—Li_3O—in the equilibrium vapor over Li_2O crystals. In 1979, Wu et al. [22] measured the ionization energy (IE) of Li_3O as 3.54±0.3 eV. In 2003, Alexandrova and Boldyrev [23] pointed out that Li_3 can be viewed as a superalkali because the IP of Li_3 is 4.08± 0.05 eV, i.e., lower than the IP of the Li atom (5.390 eV) [24]. Li_3 is a special member of superalkali families; it has three valence electrons from the three Li atoms, but loses just one to form the stable Li_3^+ cation. Li_3^+ has two valence electrons, while most superalkali cations (e.g., Li_3O^+) do not have any available valence electrons in the Li atoms.

In this work, we employed PLY radical and superalkali atoms (Li_3O and Li_3) as building blocks to assemble two complexes, designated as Li_3O-PLY and Li_3-PLY. Although

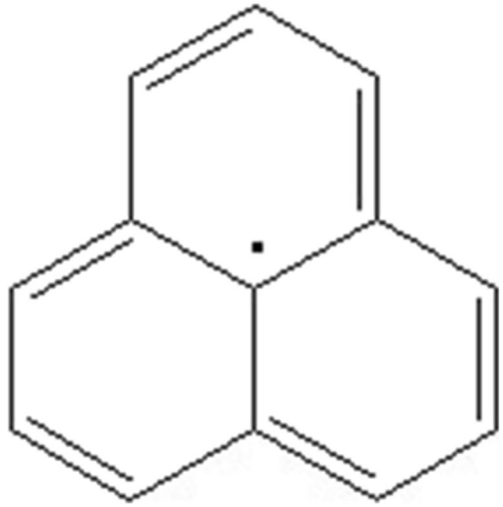

Scheme 1 Phenalenyl radical

both Li_3O and Li_3 are superalkalis, when they bond to PLY, two different types of complexes are obtained. Frontier molecular orbital (FMO) analysis has shown that Li_3-PLY has a larger diffuse electron cloud in highest-occupied molecular orbitals (HOMO; Scheme 2), which leads to larger β_0 values. Our investigation focused on the structures, bonding character, interaction energies and nonlinear optical (NLO) properties of Li_3O-PLY and Li_3-PLY.

Computational details

The hybrid meta exchange correlation functional (M06-2X) density function theory (DFT) method, has been used widely to optimize the geometries of PLY radical systems [25–30]. Besides, in our previous paper, the M06-2X method was chosen to optimize phenalenyl radical and azaphenalenyl radical [29]. Therefore, the geometrical structures of the molecules were obtained at the M06-2X/6-31+G(d) level.

Furthermore, to correct the basis set superposition error (BSSEs), the counterpoise (CP) procedure was used in calculations of interaction energies at the M06-2X/6-31+G(d) level [31, 32]. The interaction energy (E_{int}) was calculated using the following formula:

$$E_{\text{int}}(AB) = E(AB)_{AB} - \left[E(A)_{AB} + E(B)_{AB}\right] \quad (1)$$

The Wiberg bond indices (WBI) were calculated at the M06-2X/6-31+G(d) level. To calculate first hyperpolarizabilities (β_0), choosing the proper method is very important.

Specifically, considering precision and cost, the MP2 method has been proposed as the most suitable method to calculate first hyperpolarizabilities [33–35]. In the present work, the first hyperpolarizabilities were calculated at the MP2/6-31+G(d) level. For comparison, we also used the methods of M06-2X and CAM-B3LYP.

The static first hyperpolarizability was noted as:

$$\beta_0 = \left(\beta_x^2 + \beta_y^2 + \beta_z^2\right)^{1/2} \quad (2)$$

Where

$$\beta_I = \frac{3}{5}\left(\beta_{III} + \beta_{Ijj} + \beta_{Ikk}\right), I, j, k = x, y, z \quad (3)$$

In this work, the M06-2X method was also employed to evaluate NBO charge.

The hyper-Rayleigh scattering (HRS) response $\beta_{HRS}(-2\omega,\omega,\omega)$ was evaluated using the NLO Calculator program [36, 37]. The $\beta_{HRS}(-2\omega,\omega,\omega)$ is described as:

$$\beta_{HRS}(-2\omega, \omega, \omega) = \left(< \beta^2{}_{ZZZ} > + < \beta^2{}_{ZXX} \right)^{1/2} \quad (4)$$

In addition, MP2 frequency-dependent values were estimated using the multiplicative approximation given by the following equation:

$$\beta(\omega)^{MP2} \cong \beta(\omega)^{HF} \bullet \beta_0^{MP2} \Big/ \beta_0^{HF} \quad (5)$$

All calculations were performed with Gaussian 09 W program package [38].

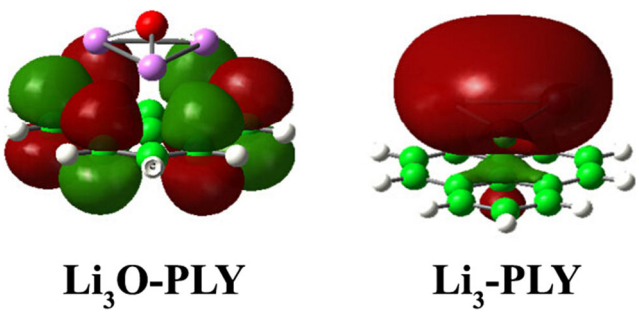

Scheme 2 Highest-occupied molecular orbitals (HOMOs) of Li_3O-PLY and Li_3-PLY

Results and discussion

Geometric structures and Wiberg bond index

The geometrical structures for Li-PLY, Li_3O-PLY and Li_3-PLY with all real frequencies are given in Fig. 1. The frequency calculations confirmed that the optimized structures were at the minimum; geometric parameters are listed in Table 1. We

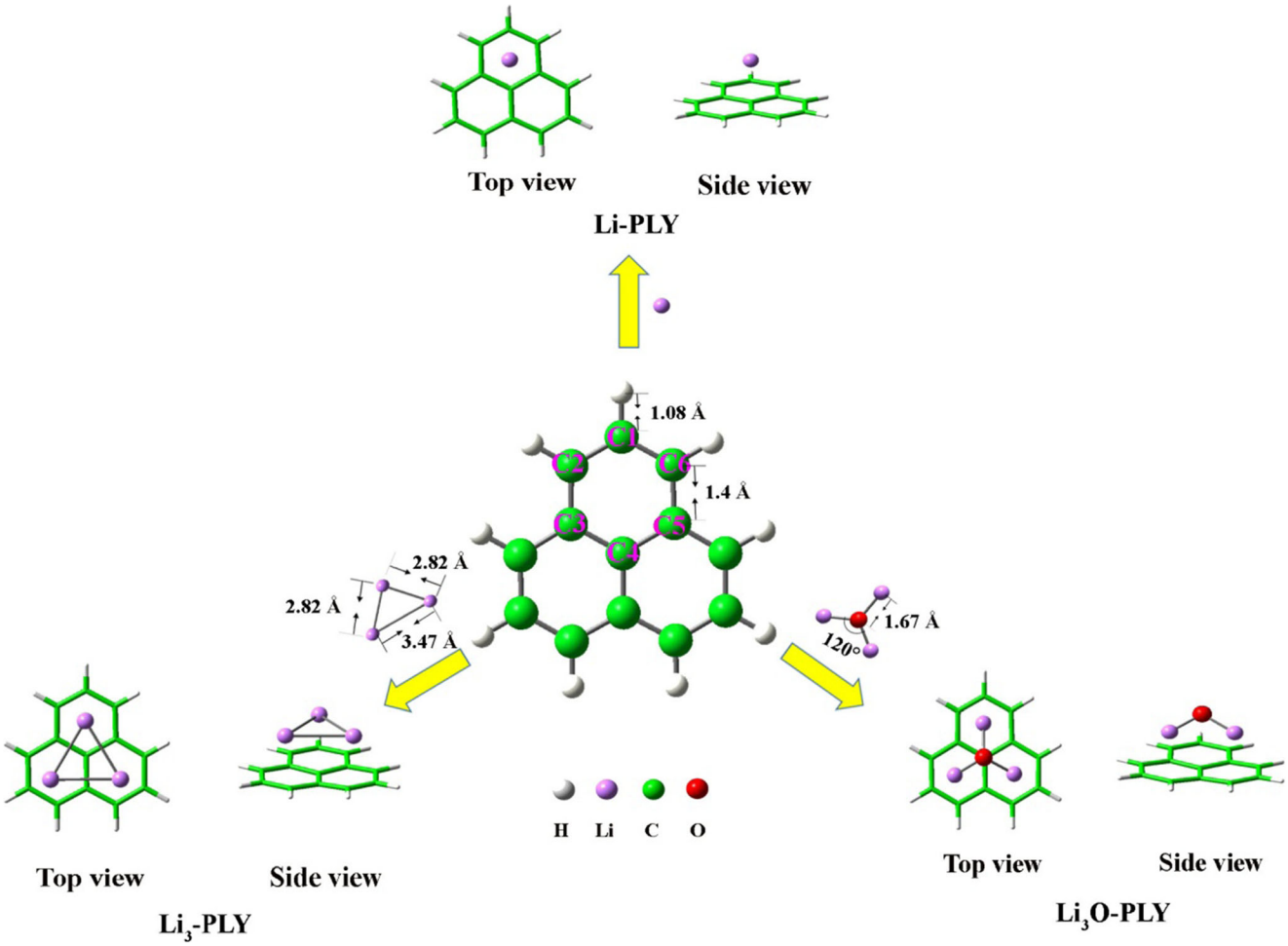

Fig. 1 Optimized structures of the three molecules and selected bond distances (Å) and bond angles (°) of phenalenyl (PLY), Li_3 and Li_3O

also calculated PLY radical, Li_3O and Li_3 (see Fig. 1). The geometric parameters were in good agreement with previously reported studies [17, 23]. As shown in Fig. 1, the structure of Li_3O is a planar triangle. However, for Li_3O-PLY, the structure of Li_3O changed to a triangle cone. For Li_3-PLY, the Li–Li distances were equal (2.725 Å), indicating that the structure of Li_3 is an equilateral triangle. However, the structure of the Li_3 monomer is that of an isosceles triangle. Hence, the bond lengths and bond angles in the complexes differ from those in monomers, which indicates that the PLY has a significant impact on the structure of Li_3O and Li_3.

Table 1 Selected bond distances (Å) and bond angles (°) of Li_3O-PLY and Li_3-PLY optimized structures at the M06-2X/6-31+G(d) level of theory

	Li_3O-PLY	Li_3-PLY
Li-C_1	2.472	2.389
Li-C_2	2.540	2.470
Li-C_3	2.702	2.688
Li-C_4	2.785	2.810
O- C_4	2.960	–
Li-O	1.707	–
Li-Li	2.945	2.725
Li-O-Li	106	–
Li-Li-Li	60	60

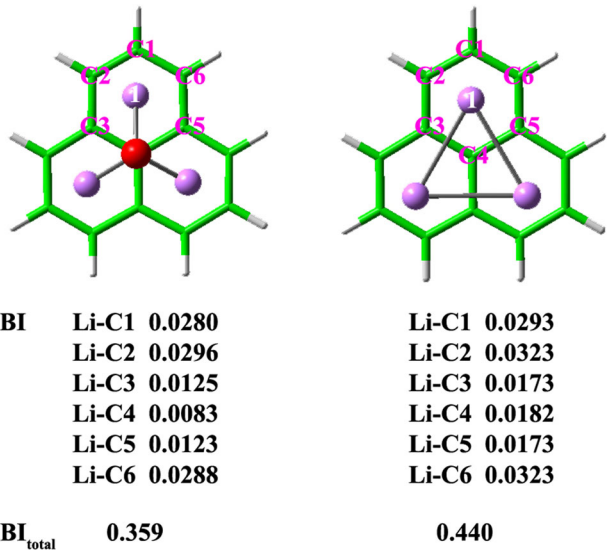

Fig. 2 Wiberg bond indices (WBI) of Li_3O-PLY and Li_3-PLY

Table 2 Interaction energies (E_{int}) and Wiberg bond indices (WBI) of Li_3O-PLY and Li_3-PLY calculated at the M06-2X/6-31+G(d) level of theory

	Li_3O-PLY	Li_3-PLY
WBI	0.359	0.441
E_{int} (kcal mol^{-1})	−72.7	−68.3

To further understand bond character, we evaluated the WBI by using the M06-2X/6-31+G(d) method (Fig. 2, Table 2). For Li_3O-PLY, the WBI value of the Li1 atom and carbon atoms in the labeled ring was 0.1195. Obviously, the three Li atoms located at the top of the three rings in the PLY plane are in the same chemical environment. Consequently, the total WBI was 0.359. Similarly, for Li_3-PLY, the total WBI was 0.440, which is larger than that of Li_3O-PLY. It is noteworthy that the increase order of WBI is inversely proportional to the distance between superalkali (Li_3O, Li_3) and PLY. This suggests that the bond in Li_3-PLY is stronger than that in Li_3O-PLY.

Natural bond orbital analysis and interaction energies

Table 3 lists the NBO charges of Li_3O, Li_3 and PLY. Clearly, the NBO charges of Li_3O (0.802) in Li_3O-PLY and Li_3 (0.777) in Li_3-PLY are close to +1. The charges of the PLYs are close to −1, which indicates electron transfer from Li_3O /Li_3 to PLY.

In order to investigate the stabilities of Li_3O-PLY and Li_3-PLY, the interaction energy (E_{int}) was calculated at the M06-2X/6-31+G(d) level of theory with CP correction, and the corresponding results are presented in Table 2. Furthermore, we used the same method to calculate the interaction energy of Li-PLY. The order of E_{int} values was Li-PLY (−49.5 kcal mol^{-1})<Li_3-PLY (−68.3 kcal mol^{-1})< Li_3O-PLY (−72.7 kcal mol^{-1}), indicating that Li_3-PLY and Li_3O-PLY are more stable in comparison with Li-PLY. Moreover, this result may help us understand the dramatic superalkali effect on E_{int} values.

Table 3 Natural bond orbital (NBO) of Li_3O-PLY and Li_3-PLY at the M06-2X/6-31+G(d) level of theory

	Li_3O-PLY	Li_3-PLY
Li	0.805	0.259
	0.805	0.259
	0.805	0.259
O	−1.613	–
Li_3O	0.802	–
Li_3	–	0.777
PLY	−0.802	−0.777

Table 4 The first hyperpolarizability (β_0, a.u.) at the MP2/6-31+G(d) level; the difference in dipole moment ($\Delta\mu$, Debye) between the ground and excited state, the transition energy (ΔE, eV) and the oscillator strength f_0 at the TD-M06-2X/6-31+G(d) level of theory

		Li3O-PLY	Li3-PLY
MP2	βx	0	15
	βy	0	12
	βz	347	5519
	β0	347	5519
M06-2X	βx	0	−300
	βy	−1	18
	βz	278	4934
	β0	278	4934
CAM-B3LYP	βx	0	13
	βy	1	17
	βz	225	5691
	β0	225	5691
TD-M06-2X	f0	0.143	0.153
	ΔE	3.28	1.95
	μe	2.30	1.53
	μg	0.84	2.12
	$\Delta\mu$a	1.46	−0.59

[a] $\Delta\mu=\mu_e-\mu_g$

Static first hyperpolarizability

The static first hyperpolarizability (β_0) of Li_3O-PLY and Li_3-PLY are given in Table 4 at the MP2, M06-2X and CAM-B3LYP level with 6-31+G(d) basis set. As shown

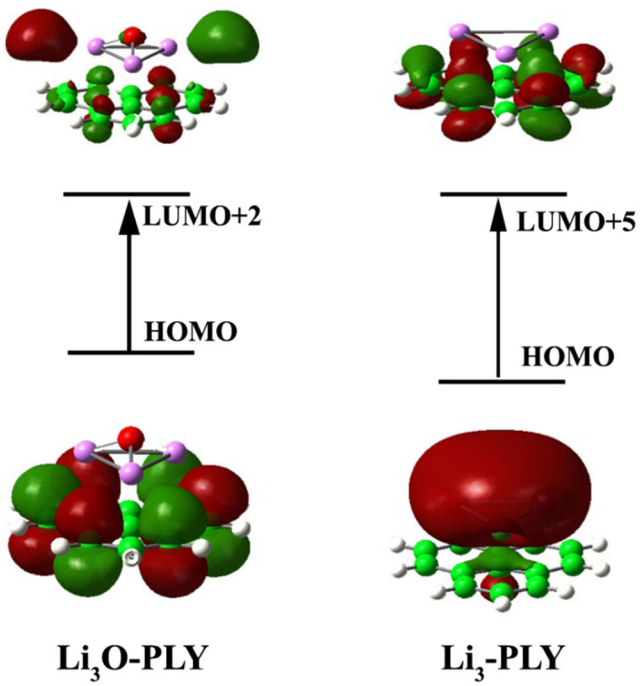

Fig. 3 Crucial transitions of Li_3O-PLY and Li_3-PLY

Table 5 Fragment contributions to highest occupied molecular orbitals (HOMOs) of Li_3O-PLY and Li_3-PLY

	Li_3O-PLY	Li_3-PLY
Li_3O (%)	2.07	–
Li_3 (%)	–	77.01
PLY (%)	97.93	22.99

in Table 4, it is clear that the $\beta_0$values calculated using the four methods are very similar. The β_0 value is 0 a.u. for an isolated PLY radical due to its centrosymmetric configuration. However, by doping Li_3O and Li_3 into PLY radical, we finally obtained two complexes (Li_3O-PLY and Li_3-PLY) without centrosymmetry. As we can see from Table 4, the β_0 values of Li_3-PLY (4943–5691 a.u.) are much larger than the value of Li_3O-PLY (225–347 a.u.). Interestingly, although two complexes are both constructed by PLY radical and superalkali atoms, the β_0 value of Li_3-PLY is dramatically larger than that of Li_3O-PLY; why?

To further understand the origin of the β_0 values, we consider the widely used two-level model [39, 40]:

$$\beta_0 \propto \frac{\Delta\mu \bullet f_0}{\Delta E^3} \tag{6}$$

Where ΔE, f_0 and $\Delta\mu$ are the transition energy, oscillator strength and difference in the dipole moments between the ground state and the crucial excited state, respectively. According to the above expression, β_0 is proportional to $\Delta\mu$ and f_0 but inversely proportional to ΔE [11–16]. The physical quantities in the two-level model may be helpful to qualitatively understand the variation in β_0 values.

In this work, the transition energies (ΔE) for Li_3O-PLY and Li_3-PLY were estimated by time-dependent (TD) M06-2X/6-31+G(d) and listed in Table 4. The order of ΔE values is Li_3O-PLY (3.28 eV)>Li_3-PLY (1.95 eV). To explain the smaller ΔE value of Li_3-PLY, we examined the HOMOs and related unoccupied molecule orbitals in Fig. 3. Clearly, Li_3-PLY has a larger diffuse electron cloud in HOMO than that of Li_3O-PLY, which makes transition easier. Therefore, the ΔE value for Li_3-PLY is smaller than the value for Li_3O-PLY, which leads to a larger β_0 value.

Furthermore, to gain insight into the detailed fragment contributions to the HOMOs of Li_3O-PLY and Li_3-PLY, we used the AOMix program [41, 42]. From Table 5, the HOMO of Li_3O-PLY is contributed mainly by PLY radical, whereas the HOMO of Li_3-PLY is contributed mainly by Li_3, which is in accordance with the HOMOs in Fig. 3. Hence, the larger contribution of Li_3 might decrease the ΔE value, whereas the larger contribution of PLY radical might increase the ΔE value. This also explains why the ΔE value of Li_3-PLY is smaller than that of Li_3O-PLY.

Absorption spectrum and frequency-dependent NLO properties

The absorption spectra of PLY, Li_3O-PLY and Li_3-PLY were simulated according to TD-M06-2X/6-31+G(d) level and the

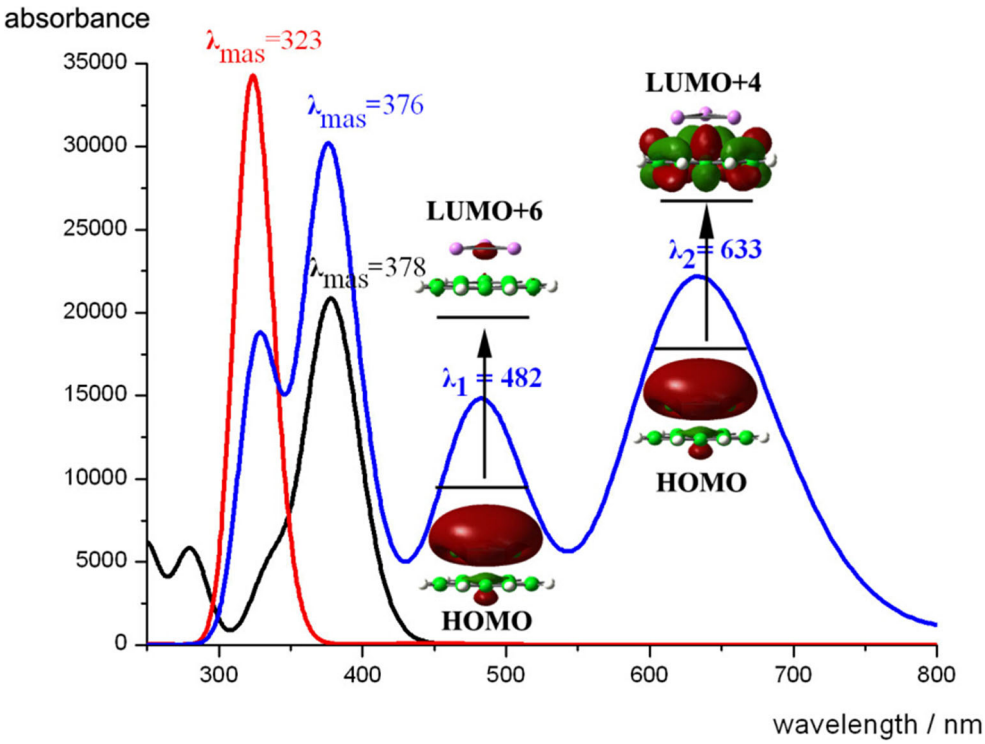

Fig. 4 Computed absorption spectra for PLY (*red*), Li_3O-PLY (*black*), Li_3-PLY (*blue*) and frontier molecular orbital (FMO) diagrams

Table 6 Wavelengths, transition energies (ΔE), oscillator strengths (f_0), dominant excitation, and the configuration interaction of Li_3-PLY at the TD-M06-2X/6-31+G(d) level of theory

λ (nm)	ΔE (eV)	f_0	Major contribution	^cC_I
485	2.56	0.1299	$H^a \rightarrow L^b$ +6	0.55
633	1.96	0.1527	H→L +4	0.46

[a] HOMO

[b] LUMO

[c] Configuration interaction

results are plotted in Fig. 4. PLY, Li_3O-PLY and Li_3-PLY have obvious absorption peaks within the visible region. Moreover, for the maximum wavelengths, Li_3O-PLY (λ_{max}=378 nm) and Li_3-PLY (λ_{max}=376 nm) display slightly bathochromic shift, compared to PLY (λ_{max}=323 nm). Interestingly, the Li_3-PLY has two new peaks at 482 and 633 nm. To further explore the new peaks, transition energies (ΔE), oscillator strengths (f_0), dominant excitation, and the configuration interaction of Li_3-PLYare listed in Table 6 and the related FMO diagrams are shown in Fig. 4. At 482 nm, the transition of Li_3-PLY occurs inside Li_3. However, at 633 nm, the transition is from Li_3 to PLY radical. Specially, the lowest energy absorption of Li_3-PLY is red-shifted to 633 nm. It may be a critically important factor that Li_3-PLY has the largest β value.

Further, in order to supply more useful information for experimentalists, the HRS response $\beta_{HRS}(-2\omega,\omega,\omega)$ was evaluated using the NLO Calculator program and coupled perturbed Hartree-Fock (CPHF) theory. In accordance with the method of calculating the static β values, we used Eq. (5) to estimate the MP2 frequency-dependent β values; the results are listed in Table 7. In accordance with the maximum absorption wavelengths of the systems, the frequency dispersion at wavelengths of 1064 nm (ω=0.0428 au), 1340 nm (ω =0.0340 au), 1460 nm (ω =0.0312 au) and 1907 nm (ω =0.0239 au) were investigated. As shown in Tables 4 and 7, the static and dynamic $\beta_{HRS}(-2\omega,\omega,\omega)$ values

Table 7 Static and dynamic (λ=0, 1907, 1460, 1340 and 1064 nm) $\beta_{HRS}(-2\omega,\omega,\omega)$ values (a.u.) of Li_3O-PLY and Li_3-PLY calculated using the MP2 and coupled perturbed Hartree-Fock (CPHF; in parentheses) methods

λ(nm)	Li_3O-PLY	Li_3-PLY
0.000	486 (231)	3564 (5854)
1907	482 (229)	6422 (10549)
1460	473 (225)	14,626 (24024)
1340	469 (223)	94,874 (155832)
1064	435 (207)	94,537 (155279)

change in the same order as the β_0 values (Li_3O-PLY<Li_3-PLY). We also found that the frequency-dependent effect was more obvious for Li_3-PLY than for Li_3O-PLY. Interestingly, for Li_3-PLY, there are two extremely large $\beta_{HRS}(-2\omega,\omega,\omega)$ values (94,874 and 94,537 a.u.) at 1340 and 1046 nm. To explain this question, let us focus on the absorption spectra (Fig. 4): there are two strong peaks at 483 and 633 nm. As a result, the two-photon resonance of Li_3-PLY is 966 and 1266 nm, which is close to 1064 and 1340 nm. It is possible that the two-photon resonance is the main reason for the very large $\beta_{HRS}(-2\omega,\omega,\omega)$ values (94,874 and 94,537 a.u.) of Li_3-PLY.

Conclusions

In the present work, we employed the PLY radical and superalkali atoms (Li_3O and Li_3) as building blocks to assemble two novel complexes, designated as Li_3O-PLY and Li_3-PLY. Our investigation focused on the structures, interaction energies, WBI and NLO properties of the two complexes. The key points of this work can be summarized as follows:

(1) The interaction energies show that Li_3O-PLY is more stable than Li_3-PLY. Moreover, Li_3-PLY and Li_3O-PLY are both more stable in comparison with Li-PLY. This result may help us understand the dramatic superalkali effect on E_{int} values.
(2) The bonding characters were investigated by NBO analysis and WBI. The results demonstrate that the bond in Li_3-PLY is stronger than the bond in Li_3O-PLY.
(3) Li_3-PLY has a larger diffuse electron cloud in HOMO than that of Li_3O-PLY, which makes transition easier. Therefore, the ΔE value for Li_3-PLY is smaller than the value for Li_3O-PLY, which leads to larger β_0 values. The order of the β_0 values is Li_3O-PLY(225–347 a.u.)<Li_3-PLY(4943–5691 a.u.).
(4) The UV–vis absorption show that the maximum wavelengths for Li_3O-PLY (λ_{max}=378 nm) and Li_3-PLY (λ_{max}=376 nm) display a slight bathochromic shift compared to PLY (λ_{max}=323 nm).

We expect that this work could provide guidance for theoretical and experimental scientists attempting to design novel NLO materials with PLY and superalkali.

Acknowledgments The authors gratefully acknowledge the financial support from National Science Foundation of China (NSFC) (21003019, 21473026), the Science and Technology Development Planning of Jilin Province (201201062 and 20140101046JC), the Computing Center of Jilin Province provided essential support and H.-L.X. acknowledges support from the Hong Kong Scholars Program And Project funded by the China Postdoctoral Science Foundation (2014 M560227).

References

1. Suzuki S, Morita Y, Fukui K, Sato K, Shiomi D, Takui T, Nakasuji K (2006) Aromaticity on the pancake-bonded dimer of neutral phenalenyl radical as studied by MS and NMR spectroscopies and NICS analysis. J Am Chem Soc 128:2530
2. Huang J, Kertesz M (2007) Intermolecular covalent π–π bonding interaction indicated by bond distances, energy bands, and magnetism in biphenalenyl biradicaloid molecular crystal. J Am Chem Soc 129:1634
3. Craciun S, Donald KJ (2009) Radical bonding: structure and stability of bis(phenalenyl) complexes of divalent metals from across the periodic table. Inorg Chem 48:5810
4. Small D, Rosokha SV, Kochi JK, Head-Gordon M (2005) Characterizing the dimerizations of phenalenyl radicals by ab initio calculations and spectroscopy: σ-bond formation versus resonance π-stabilization. J Phys Chem A 109:11261
5. Nakano M, Takebe A, Kishi R, Fukui H, Minami T, Kubota K, Takahashi H, Kubo T, Kamada K, Ohta K, Champagne B, Botek E (2008) Intermolecular interaction effects on the second hyperpolarizability of open-shell singlet diphenalenyl radical dimer. Chem Phys Lett 454:97
6. Chi X, Itkis ME, Patrick BO, Barclay TM, Reed RW, Oakley RT, Cordes AW, Haddon RC (1999) The first phenalenyl-based neutral radical molecular conductor. J Am Chem Soc 121:10395
7. Itkis M, Chi X, Cordes A, Haddon R (2002) Magneto-optoelectronic bistability in a phenalenyl-based neutral radical. Science 296:1443
8. Cyrański MK, Havenith RWA, Dobrowolski MA, Gray BR, Krygowski TM, Fowler PW, Jenneskens LW (2007) The phenalenyl motif: a magnetic chameleon. Chem Eur J 13:2201
9. Ueda A, Wasa H, Suzuki S, Okada K, Sato K, Takui T, Morita Y (2012) Chiral stable phenalenyl radical: synthesis, electronic-spin structure, and optical properties of [4]helicene-structured diazaphenalenyl. Angew Chem-Int Edit 51:6691
10. Sarkar A, Itkis ME, Tham FS, Haddon RC (2011) Synthesis, structure, and physical properties of a partial π-stacked phenalenyl-based neutral radical molecular conductor. Chem Eur J 17:11576
11. Li Z-R, Wang F-F, Wu D, Li Y, Chen W, Sun X-Y, Gu FL, Aoki Y (2006) Royal crown-shaped electride Li_3-N_3-Be containing two superatoms: new knowledge on aromaticity. J Comput Chem 27:986
12. Wang B-Q, Li Z-R, Wu D, Wang F-F (2007) Structures and static electric properties of novel alkalide anions F-Li+Li- and $F^-Li_3^+Li_3$. J Phys Chem A 111:6378
13. Tong J, Li Y, Wu D, Wu Z-J (2012) Theoretical study on polynuclear superalkali cations with various functional groups as the central core. Inorg Chem 51:6081
14. Tong J, Wu Z, Li Y, Wu D (2013) Prediction and characterization of novel polynuclear superalkali cations. Dalton T 42:577
15. Cochran E, Meloni G (2014) Hypervalence in monoxides and dioxides of superalkali clusters. J Chem Phys 140:204–319
16. Sun W-M, Fan L-T, Li Y, Liu J-Y, Wu D, Li Z-R (2014) On the potential application of superalkali clusters in designing novel alkalides with large nonlinear optical properties. Inorg Chem 53:6170
17. Yokoyama K, Tanaka H, Kudo H (2001) Structure of hyperlithiated Li_3O and evidence for electronomers. J Phys Chem A 105:4312
18. Đustebek J, Veličković S, Veljković F, Veljković M (2012) Production of heterogeneous superalkali clusters LinF (n = 2–6) by knudesn-cell mass spectrometry. Dig J Nano Mater Bios 7:1365
19. Li Y, Wu D, Li Z-R (2008) Compounds of superatom clusters: preferred structures and significant nonlinear optical properties of the BLi6-X (X = F, LiF2, BeF3, BF4) motifs. Inorg Chem 47:9773
20. Tong J, Li Y, Wu D, Li Z-R, Huang X-R (2011) Ab initio investigation on a new class of binuclear superalkali cations $M_2Li_2k^+1^+$ ($F_2Li_3^+$, $O_2Li_5^+$, $N_2Li_7^+$, and $C_2Li_9^+$). J Phys Chem A 115:2041
21. Kudo H, Wu CH, Ihle HR (1978) Mass-spectrometric study of the vaporization of Li_2O(s) and thermochemistry of gaseous LiO, Li_2O, Li_3O, and Li_2O_2. J Nucl Mater, J 78:380
22. Wu CH, Kudoa H, Ihle HR (1979) Thermochemical properties of gaseous Li_3O and Li_2O_2. J Chem Phys 70:1815
23. Alexandrova AN, Boldyrev AI (2003) σ-Aromaticity and σ-antiaromaticity in alkali metal and alkaline earth metal small clusters. J Phys Chem A 107:554
24. Karplus M, Porter RN (1970) Atoms and molecules; an introduction for students of physical chemistry. Benjamin, New York
25. Zhong R-L, Zhang J, Muhammad S, Hu Y-Y, Xu H-L, Su Z-M (2011) Boron/nitrogen substitution of the central carbon atoms of the biphenalenyl diradical π dimer: a novel 2e–12c bond and large NLO responses. Chem Eur J 17:11773
26. Tian Y-H, Huang J, Kertesz M (2010) Fluxional [sigma]-bonds of 2,5,8-tri-tert-butyl-1,3-diazaphenalenyl dimers: stepwise [3,3], [5, 5] and [7,7] sigmatropic rearrangements via [small pi]-dimer intermediates. Phys Chem Chem Phys 12:5084
27. Tian Y-H, Kertesz M (2010) Is there a lower limit to the CC bonding distances in neutral radical π-dimers? The case of phenalenyl derivatives. J Am Chem Soc 132:10648
28. Sini G, Sears JS, Brédas J-L (2011) Evaluating the performance of DFT functionals in assessing the interaction energy and ground-state charge transfer of donor/acceptor complexes:tetrathiafulvalene − tetracyanoquinodimethane (TTF−TCNQ) as a model case. J Chem Theory Comput 7:602
29. Zhong R-L, Xu H-L, Sun S-L, Qiu Y-Q, Zhao L, Su Z-M (2013) Theoretical investigation on the 2e/12c bond and second hyperpolarizability of azaphenalenyl radical dimers: strength and effect of dimerization. J Chem Phys 139, 124314
30. Chen S, Sun S-L, Wu H-Q, Xu H-L, Zhao L, Su Z-M (2014) Superatoms (Li_3O and BeF_3) induce phenalenyl radicalπ–dimer: fascinating interlayer charge-transfer and large NLO responses. Dalton T 43:12657
31. Alkorta I, Elguero J (1998) Theoretical study of strong hydrogen bonds between neutral molecules:the case of amine oxides and phosphine oxides as hydrogen bond acceptors. J Phys Chem A 103:272–279
32. Boys SF, Bernardi F (1970) The calculation of small molecular interactions by the differences of separate total energies. Some procedures with reduced errors. Mol Phys 19:553–566
33. Chen W, Li Z-R, Wu D, Li Y, Sun C-C, Gu FL (2005) The structure and the large nonlinear optical properties of Li@Calix[4]pyrrole. J Am Chem Soc 127:10977–10981
34. Xu H-L, Li Z-R, Wu D, Wang B-Q, Li Y, Gu FL, Aoki Y (2007) Structures and large NLO responses of new electrides: Li-doped fluorocarbon chain. J Am Chem Soc 129:2967
35. Muhammad S, Xu H, Liao Y, Kan Y, Su Z (2009) Quantum mechanical design and structure of the $Li@B_{10}H_{14}$ basket with a remarkably enhanced electro-optical response. J Am Chem Soc 131:11833
36. Dongdong Qi. NLO Calculator, Version 0.2. University of Science and Technology Beijing, Beijing 100083, China
37. Zhang L, Qi D, Zhao L, Chen C, Bian Y, Li W (2012) Density functional theory study on subtriazaporphyrin derivatives: dipolar/octupolar contribution to the second order nonlinear optical activity. J Phys Chem A 116:10249
38. Frisch MJ, Trucks GW, Schlegel HB et al (2009) Gaussian 09, revision A.02; Gaussian, Inc. Wallingford, CT
39. Oudar JL, Chemla DS (1977) Hyperpolarizabilities of the nitroanilines and their relations to the excited state dipole moment. J Chem Phys 66:2664

40. Oudar JL (1977) Optical nonlinearities of conjugated molecules. Stilbene derivatives and highly polar aromatic compounds. J Chem Phys 67:446
41. Gorelsky SI (2009) AOMix version 6.46: program for molecular orbital analysis, University of Ottawa. Available at: http://www.sg-chem.net/
42. Gorelsky SI, Lever ABP (2001) J Organomet Chem 635:187